

**D. M. Gorinevsky**  
**A. Yu. Shneider**

Institute for Problems of Information Transmission  
Academy of Sciences of the USSR  
Moscow, USSR

# Force Control in Locomotion of Legged Vehicles over Rigid and Soft Surfaces

## Abstract

*The control system of the hexapod walking vehicle, designed at the Institute for Mechanics at Moscow State University and at the Institute for Problems of Information Transmission at the USSR Academy of Sciences, is extended to effect the control of foot-contact forces and locomotion in soft soil. The previously developed positional control system enables the computation of commanded motion of the vehicle legs and positional feedback to track this commanded motion. Force feedback is added to the control system, in addition to computation of commanded forces and leg position corrections for leg sinkage during soft soil locomotion.*

*Such an elaborate control system has made it possible to solve the problems of controlling the distribution of vertical foot force components in locomotion over a rigid surface and of foot-force vectors in locomotion between planes forming a dihedral angle. A number of algorithms are proposed to control vertical force components (loads on legs) and leg sinkage in locomotion in elastic and consolidating soils. In the latter case, which corresponds to most natural soils, the bearing properties of the surface are considered a priori unknown.*

*The results of the experimental implementation of the algorithms are presented.*

## Introduction

A multi-leg walking vehicle is a mechanical system statically indeterminate with respect to forces acting on its legs (foot forces). The control of these forces makes it possible to reduce the antagonism among the

legs, loads on the vehicle structure, and energy consumption. Force control is needed to raise the adaptability of the vehicle to irregular terrain and different types of soil. For instance, in locomotion over complex terrain, the necessity may arise to control the horizontal force components so that contact forces are within friction cones. In locomotion in soft soil, it is necessary to control loads on the legs because of their sinkage into soil.

The possibility of force distribution control in a walking vehicle has been discussed for a few years. There are a number of approaches to the distribution problem based on different criteria. At present it is clear that the realization of force distribution calculated by any method requires that the vehicle legs should be equipped with force sensors and that force feedback should be introduced into the control circuit. Such an approach is widely used in manipulator systems (Whitney 1977). In at least two existing walking vehicles, the legs are equipped with force sensors (Gurfinkel et al 1981; Klein and Briggs 1980). However, the authors do not know any work on experimental realization of force distribution control in legged locomotion. This seems to be a result of the complexity of the legged locomotion problem and the necessity to compute force distribution in real time and to process simultaneously a large amount of sensory information. The questions concerning the control of vehicle motion in soft soil are closely connected with the force control problem, yet these questions have been investigated poorly.

The aim of our work was to develop and experimentally check the algorithms of force control during locomotion in different situations, including walking in soft soil.

The development of algorithms and their experimental investigation require a walking vehicle with an advanced control system. The control system must

Fig. 1. Coordinate system, leg numbering, and vehicle dimensions.

allow extension (i.e., the addition of the control of forces and leg sinkage in soft soil locomotion). Experiments were carried out on a hexapod vehicle and control system designed by the Institute for Mechanics at Moscow State University (IM MSU) and the Institute for Problems of Information Transmission at the USSR Academy of Sciences (IPIT, USSR Acad. Sci.) (Devjanin et al. 1983, 1987; Gurfinkel et al. 1981, 1982). This control system fully meets the above requirements.

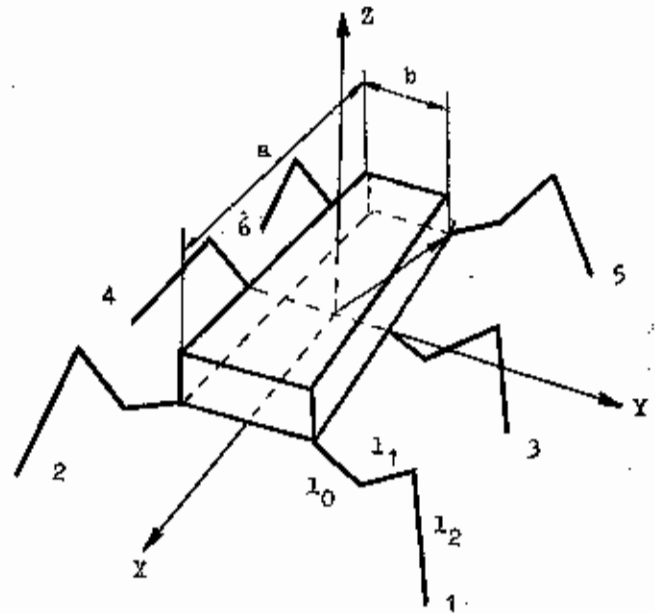
The upper level of the control system prescribes the global motion parameters. The lower level ensures a regular walking pattern in accordance with these parameters. The previously developed positional control system provides the computation of the commanded position of the legs and position feedback to track the commanded positions. In our work, force feedback and two computational processes (computation of commanded forces in the legs and correction of the leg positions for the amount of sinkage into soft soil) are added to the control system. The special feature of the algorithms of force distribution is the use of a smooth redistribution of forces when the set of supporting legs is changed.

## 1. A Walking Vehicle and Its Control System

The description of the hexapod vehicle used in the research is given in greater detail elsewhere (Devjanin et al. 1982, 1983, 1987; Gurfinkel et al. 1981, 1982).

### 1.1. Vehicle Design

The vehicle has six identical legs, with three powered degrees of freedom each. Three-component force sensors using strain-gauges are mounted in the shanks (Devjanin et al. 1982). Each ankle rotates passively



with three degrees of freedom, and each foot is equipped with a ground contact sensor. The legs are powered by electric drives with gear reducers and are equipped with joint angle potentiometer sensors.

The vehicle body carries a gyroscopic attitude sensor to measure the pitch and roll angles of the body. The distance from the body to the supporting surface (i.e., the clearance) was measured in our experiments by means of an infrared proximity sensor mounted on the body. During soft soil locomotion, a narrow flat board with known albedo was placed on the soil beneath the sensor path to ensure clearance recording.

Fig. 1 shows the numbering of the legs and a body-fixed coordinate system with origin at the body center. The  $OX$  axis is in the direction of progression, the  $OZ$  axis is perpendicular to the plane passing through the leg suspension points, and the  $OY$  axis completes a right-handed set.

The main geometric and mass parameters of the vehicle are as follows: the body length  $a = 700$  mm; its width (distance between the leg suspension points)  $b = 210$  mm; lengths of the leg links  $l_0 = 75$  mm,  $l_1 = 100$  mm,  $l_2 = 170$  mm; total mass of the vehicle is 22 kg; leg mass is 2.7 kg.

## 1.2. Control System

First we consider the operation of the positional control system used in our experiments.

The upper level of the control system is supervisory. It prescribes such motion parameters as a gait pattern, track width, clearance, and the locomotion cycle parameters. A human operator also controls, with the aid of the control handle, the components  $v_x$ ,  $v_y$  of the linear velocity and the component  $\omega_z$  of the angular velocity of the vehicle body.

The operation of the control system is based on the assumption that the motion is slow enough to be described at the kinematic level. For this reason the control system consists mainly of the units that compute the commanded motion of the vehicle legs. The tip of each leg moves relative to the body along a closed trajectory called the locomotion cycle. For each leg, the transfer and support phases alternate.

Within the part of the locomotion cycle called the adaptation zone, the leg lowering ceases when the ground contact sensor touches the support, and the leg goes to the support phase. The adaptation zone dimension is set to be about 20% of the shank length.

By coordinating the locomotion cycle phases in different legs, it is possible to obtain different gait patterns. The control system provides regular gaits (i.e., the gaits in which the transfer from one leg set to another is separated by the joint support phase; all the legs provide support). The existence of the joint support phase is very important in this work. This phase enables the redistribution of the foot forces during locomotion when all the legs are on the supporting surface.

The motion of each leg during the support phase is specified to provide a desired body motion. The leg tip coordinates and the linear  $v$  and angular  $\omega$  velocities of the body uniquely determine the leg tip velocity.

Note that the commanded motion of a leg tip is calculated in the body-fixed Cartesian coordinates. The commanded joint angles are calculated by a hardware resolver that converts the leg tip coordinates to the joint angles. In the analog servosystem, the difference between the commanded joint angle and the angle determined by the potentiometer is used to generate the control voltage.

## 2. Force Control

This section is concerned with improvements made in the control system to make it possible to control foot forces during locomotion.

### 2.1. Active Compliance

First consider the method of controlling the foot forces. The method consists of equipping each leg with a force sensor and feeding the signals of these sensors to the control loop.

In order to understand the behavior of a system with force feedback, suppose that the servosystems track the commanded coordinates of the leg tips to a high degree of accuracy. Write the radius vector  $r^{(i)}(x^{(i)}, y^{(i)}, z^{(i)})$  of the  $i$ th leg in the body-fixed coordinate system as  $r^{(i)} = r_*^{(i)} + \delta r^{(i)}$ , where  $r_*^{(i)}$  is the commanded position calculated by the leg motion control algorithms. Because of force feedback, the positional servosystem receives the leg position, which differs from  $r_*^{(i)}$  by

$$\delta r^{(i)} = \Lambda^{(i)}(N^{(i)} - N_*^{(i)}), \quad (1)$$

where  $\Lambda^{(i)}$  is the symmetric positive definite feedback gain matrix,  $N_*^{(i)}$  is a command force vector. If the measured force  $N^{(i)}$  coincides with the commanded force  $N_*^{(i)}$ , the leg tip position  $r^{(i)}$  is equal to the commanded value  $r_*^{(i)}$ . If the force acting on the leg differs from the commanded value, it causes an additional leg displacement proportional to the difference. Such a behavior of the system similar to that of an elastic spring with a compliance  $\Lambda^{(i)}$  is called active compliance (Devjanin et al. 1982; Klein and Briggs 1980). Active compliance can be controlled by varying the elements of the matrix  $\Lambda^{(i)}$ .

In the absence of active compliance, force distribution in a statically indeterminate multileg system depends on unknown elastic properties of the leg structure and is greatly influenced by small errors of tracking and computing the commanded leg positions. In the presence of active compliance, this distribution

Fig. 2. Interaction of the positional and force parts of the control system.

is determined by the matrices  $A^{(l)}$  and commanded forces  $N_*^{(l)}$ . If compliance is sufficiently high, small positioning errors have no noticeable effect on the force distribution. In this case the forces  $N^{(l)}$  are equal to the commanded forces  $N_*^{(l)}$  if the latter satisfy the static equilibrium equations.

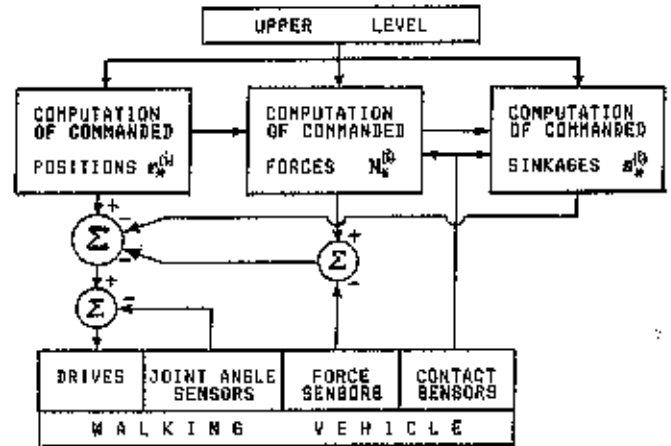
For force distribution control on the basis of active compliance, some new units are installed into the lower level of the control system. The functions of these units are similar to those of the positional part of the control system. These are computation of the commanded forces  $N_*^{(l)}$  and implementation of force feedback to track the commanded forces. The positional and "force" parts of the control system interact because they control the same object. This interaction results in the correction of the commanded leg position as a result of force feedback (1).

The force feedback loop is closed with the aid of a hardware unit implemented primarily with analog facilities. This unit compensates for the zero drift of the force sensors, stores their force readings into the analog memory at the transfer phase of a given leg, and converts force data from sensor coordinates to body coordinates. This unit also includes the circuits generating the corrections  $\delta r^{(l)}$  in eq. (1) to the commanded trajectories of the legs. Because of the hardware implementation, the delay in the feedback loop was reduced to 1 ms.

The algorithms used to compute the commanded forces are rather complicated and may vary depending on the situation. The algorithms allow for a longer computational delay. For this reason it is better to compute the commanded forces using digital facilities (for example, a separate microprocessor). In our experiments a Nova 2/10 minicomputer was used for the purpose.

In the case of soft soil locomotion, it is necessary to correct the position of each leg for its sinkage. In our experiments computation of the sinkage correction for the commanded leg position  $s_*^{(l)}$  is a separate process carried out along with the computation of the commanded position  $r_*^{(l)}$  and commanded force  $N_*^{(l)}$ . The computation of the leg sinkage is closely related to the computation of forces. The interaction of the above control processes is described by the equation

$$r^{(l)} = r_*^{(l)} + A^{(l)}(N^{(l)} - N_*^{(l)}) + s_*^{(l)} \quad (2)$$



which replaces eq. (1). In our experiments the sinkage  $s_*^{(l)}$  and the commanded forces  $N_*^{(l)}$  were calculated by the same computer.

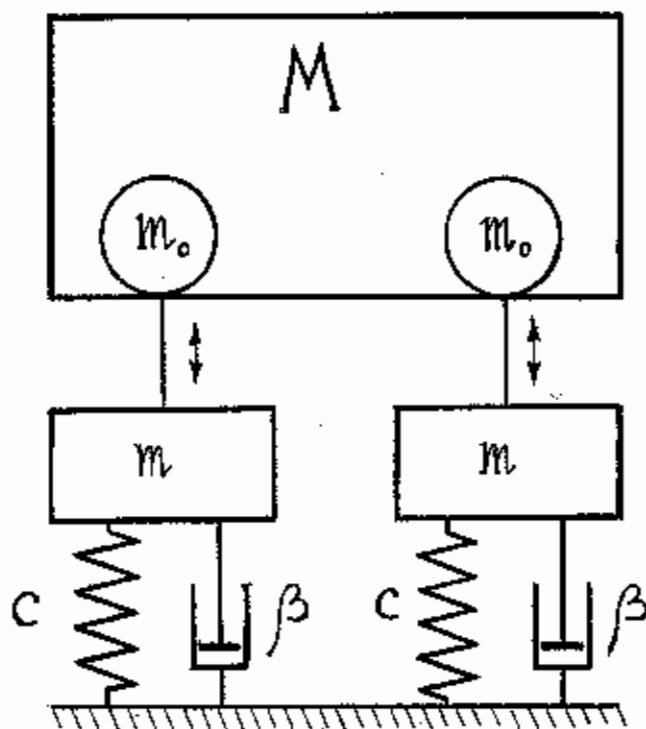
The three interacting processes described are schematically shown in Figure 2. The forces and leg sinkages are controlled at the lower level. Accordingly, the algorithms used should be based on the lower-level information about the current configuration of the vehicle and global parameters of its motion. These algorithms must not use the information about the subsequent motion prescribed by the upper level. Such a structure of the control system enables the upper level (i.e., a human operator) to guide the vehicle without paying attention to force distribution and leg sinkage, which are automatically controlled at the lower level.

We now consider in greater detail both the force feedback and force command computation. The next subsection is concerned with the transient process dynamics in the presence of force feedback. The remainder of the paper is devoted to the software-implemented algorithms for computation of the commanded forces and leg sinkage.

## 2.2. Transient Process Dynamics

The concept of active compliance is based on the assumptions that the commanded positions are served to a high degree of accuracy and transient processes in

Fig. 3. Simple mechanical model for the dynamics of legged vehicle with force feedback.



the system decay quickly. Such a quasi-static consideration helps to understand the behavior of a system with force feedback. However, it may happen that the steady state is unstable, and undamped vibrations occur in the system. Such vibrations are observed in experiments at certain feedback gains. Let us proceed with an analysis of the transient process dynamics in the walking vehicle under force feedback control.

#### Mathematical Model

We restrict ourselves to a simplified mathematic model that reflects the main features of the system dynamics. A more advanced model is treated elsewhere (Gorinevsky and Shneider 1987).

A schematic of the model is shown in Figure 3. The system consists of a vertically moving vehicle body of mass  $M$  with two legs, each of mass  $m$ , that can move downward. The lumped mass  $m_0$  is a result of the dynamics of the rotors in the electric drive or of the fluid in the hydraulic drive. Each leg is equipped with

a force sensor that is modeled by a massless force-measuring spring element and a dashpot. The system is provided with position and force feedback.

Now proceed with the governing equations. Let us consider transient processes in the vicinity of the system steady state. Let  $q$  be the vertical displacement of the body from the steady state,  $x_i (i = 1, 2)$  be the drive-controlled displacement of the legs relative to the body,  $y_i (i = 1, 2)$  be the displacement of the legs in the earth-fixed coordinate system caused by the spring deformation. These displacements are evidently related:

$$x_i = q - y_i. \quad (3)$$

To construct the Lagrange equations we need the kinetic energy of the system

$$T = \frac{1}{2} M \dot{q}^2 + \frac{1}{2} m_0 (\dot{x}_1^2 + \dot{x}_2^2) + \frac{1}{2} m (\dot{y}_1^2 + \dot{y}_2^2). \quad (4)$$

The first term in eq. (4) is the kinetic energy of the vehicle body, the second term represents the energy of the drive rotors, and the third term is the leg kinetic energy.

The deviation of the potential energy from its stationary value is caused by the spring element deformation

$$\Pi = \frac{1}{2} c (y_1^2 + y_2^2). \quad (5)$$

Energy dissipation in the structure is described by the dissipative function

$$R = \frac{1}{2} b (\dot{y}_1^2 + \dot{y}_2^2) \quad (6)$$

Variations of the gravity forces are zero. Now let us consider the control forces—more precisely, deviations of these forces from their stationary values proportional to the control voltage. The voltage is generated by the positional servosystem; therefore

$$Q_i = -G(x_i - \delta x_i) - b_0 \dot{x}_i \quad (i = 1, 2), \quad (7)$$

where  $G$  is the positional feedback gain,  $b_0 \dot{x}_i$  is the force caused by the back e.m.f. (the term taking ac-

count of the tachometer feedback is of the same form),  $\delta x_i$  is the deviation from the commanded value of the leg position. This deviation is caused by force feedback, in accordance with eq. (1). Thus,

$$\delta x_i = \Lambda N_i, \quad (i = 1, 2), \quad (8)$$

where  $\Lambda$  is the active compliance value,  $N_i = cy_i$  is the deviation of the force from the stationary value. Subject to eq. (8), eq. (7) may be written as

$$Q_i = -Gx_i - b_0x_i - kN_i, \quad N_i = cy_i, \quad (9)$$

where  $k = \Lambda G$  is the force feedback dimensionless gain.

Using eqs. (3)–(6) and (9), construct Lagrange's equations with respect to the coordinates  $q$  and  $x_i (i = 1, 2)$ . Substituting  $y_i$  for  $x_i$  in these equations we obtain in accordance with eq. (3):

$$\begin{aligned} M\ddot{q} + m(\dot{y}_1 + \dot{y}_2) + b(y_1 + y_2) + c(y_1 + y_2) &= 0 \\ -(m_0\ddot{q} + b_0\dot{q} + Gq) + (m_0 + m)\dot{y}_i + (b_0 + b)y_i & \\ + [c(1+k) + G]y_i = 0 \quad (i = 1, 2) & \end{aligned} \quad (10)$$

### 2.2.2. Fast and Slow Motions

Consider the new variables  $Y = (y_1 + y_2)/2$  and  $X = y_1 - y_2$ . Then the equations in eq. (10) separate into two groups. The first group of equations describes the interrelated motions of the vehicle body and legs

$$M\ddot{q} + 2m\dot{Y} + 2bY + 2cY = 0$$

$$-(m_0\ddot{q} + b_0\dot{q} + Gq) + (m + m_0)\dot{Y} + (b + b_0)Y + [c(1+k) + G]Y = 0 \quad (11)$$

The separated equation describes the motion of the legs, within the framework of static indeterminacy, which produces no resultant force acting on the body

$$(m + m_0)\dot{X} + (b + b_0)X + [c(1+k) + G]X = 0 \quad (12)$$

It can be shown that the characteristic equation of system (11) satisfies the Hurwitz conditions, and consequently, the system is stable. Equation (12) is an equation of damped vibrations and is also stable.

Suppose that the elastic element of the force sensor is "rigid." This may be considered to hold in practice.

Let

$$c = \lambda^2 c_1, \quad b = \lambda b_1, \quad \epsilon = 1/\lambda \ll 1, \quad (13)$$

where  $\lambda$  is a large parameter,  $\epsilon$  is a small parameter, and  $c_1$  and  $b_1$  are of the order of magnitude of unity. Such an introduction of the large parameter corresponds to an approximately constant decrement of vibrations in the structure as its stiffness increases.

Subject to eq. (13), the system of equations (11), (12) is singularly perturbed. In this system  $X, \dot{X}, Y, \dot{Y}$  are fast variables and  $q$  and  $\dot{q}$  are slow variables. To separate motions with respect to these variables, eqs. (11) and (12) should be expressed in accordance with Tikhonov (1952) in the state form by introducing the variables  $V_x = \epsilon \dot{X}$ ,  $V_y = \epsilon \dot{Y}$ , and  $V_q = \dot{q}$ . As a result, we obtain the boundary layer system describing "fast" motions.

$$\begin{aligned} \left[ \frac{M}{2}(m + m_0) + mm_0 \right] \dot{V}_y + \lambda b_1 \left( \frac{M}{2} + m_0 \right) V_y & \\ + \lambda^2 c_1 \left[ \frac{M}{2}(1+k) + m_0 \right] V_y = 0 & \\ (m + m_0)\dot{X} + \lambda b_1 X + \lambda^2 c_1 (1+k)X = 0 & \end{aligned} \quad (14)$$

and the reduced system, which describes "slow" motions

$$\left[ \frac{M}{2}(1+k) + m_0 \right] \dot{q} + b_0 \dot{q} + Gq = 0 \quad (15)$$

Equations (14) and (15) describe damped oscillations. Increasing the force feedback gain  $k$  the frequency of fast motions (14) rises as  $k^{1/2}$ , and the damping decrement decreases as  $k^{-1/2}$ . The frequency of slow motions (15) and the damping decrement decrease as  $k^{-1/2}$ . Accordingly with increasing  $k$ , the oscillations in the system damp slower. An analysis of a more detailed model of the system given elsewhere (Gorinevsky and Shneider 1987) shows that with increasing  $k$ , both fast and slow motions become unstable.

### Comparison with Experiment

Now let us compare the model with experimental results obtained on the IM-IPIT hexapod vehicle. Each

**Table 1. Model Parameters Corresponding to the Experimental Vehicle**

$M$	$m$	$m_0$	$b_0$	$c$	$b$	$G$
10	5	$3 \cdot 10^3$	$9 \cdot 10^4$	$15 \cdot 10^4$	$10^5$	$4 \cdot 10^5$

leg in the model corresponds to half of the vehicle legs (three legs). The model parameters, which approximately correspond to the experimental vehicle, are given in Table 1. The values are expressed in SI.

In our experiments the force feedback gain  $k$  was set to different values in the range 80–300.

First consider fast motions. As can be seen from Table 1, the effective mass  $m_0$  caused by the rotor dynamics is much larger than the other masses in the system. The product  $kM$  is of the same order. Therefore, in accordance with eq. (14), the damping of vibrations along the  $X$  coordinate is the lowest. These vibrations describe force redistribution among the supporting legs. The decrement for  $k = 320$  is less than the initial decrement by a factor of  $k^{1/2} \approx 18$ . At  $k = 320$ , eq. (14) gives the frequency of these vibrations

$$\nu = 1/(2\pi) \cdot [kc/(m + m_0)]^{1/2} = 15.5 \text{ Hz.}$$

At large values of force gain ( $k \approx 300$ – $400$ ), small-magnitude vibrations with a frequency of about 12 Hz were observed in experiments. These vibrations may be supposed to correspond to fast motions in the model considered.

Now proceed with slow motions (15). These are motions of the vehicle with actively compliant legs. An increase in  $k$  behaves as if there were a rise in the vehicle inertia. This rise is not very noticeable because of a large inertia  $m_0$  of the drive (at  $k = 300$ ,  $Mk/2 \approx 1500$ , and  $m_0 \approx 3000$ ). The frequency of slow motions is

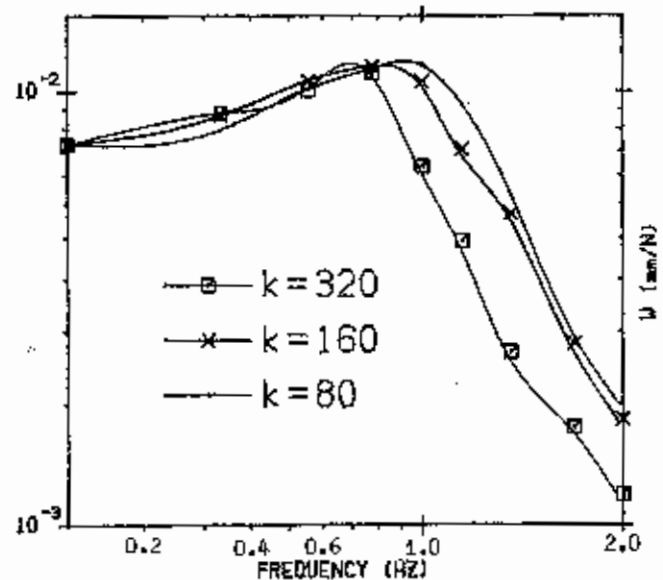
$$\nu = 1/(2\pi) \cdot [G/(Mk/2 + m_0)]^{1/2} \approx 1.5 \text{ Hz,}$$

the damping coefficient is

$$\zeta = b[(Mk/2 + m_0)G]^{-1/2} \approx 2.$$

Thus, slow motions are strongly damped. For the sake of comparison with theory, the system frequency re-

**Fig. 4. Experimental magnitude-vs.-frequency plots of vehicle pitch vibrations.**



sponse was obtained. For this purpose a disturbing harmonic voltage was applied to the drives. This voltage was distributed among the legs so that several modes of vehicle vibrations might occur. The magnitude of the vibrations of the vehicle body at a certain point was measured.

If the harmonic disturbance force acting in the drive is taken into account in the mathematic model, then the reduced system describing motions for long time intervals assumes the form

$$\left[ \frac{M}{2} (1 + k) + m_0 \right] \ddot{q} + b\dot{q} + Gq = F_0 \sin(\omega t)$$

The amplitude of body vibrations is

$$q_0 = W(\omega)F_0, \quad W(\omega) = \left[ \left( \omega^2 \left( \frac{M}{2} (1 + k) + m_0 \right) - G \right)^2 + b_0^2 \omega^2 \right]^{-1/2} \quad (16)$$

where  $W(\omega)$  is the frequency response of the system.

Experimentally obtained magnitude-vs.-frequency plots are shown in Figure 4. The natural frequency of the system is about 1 Hz, and the damping coefficient  $\zeta \approx 1.4$ , this being close to the theoretical estimate. As can be seen from Figure 4, an increase in  $k$  leads to a decrease in the magnitude at high frequencies, in

agreement with eq. (16). A relatively slight change in the form of the magnitude-vs.-frequency plot with increasing  $k$  can be explained by the fact that the effective mass  $m_0$  of the rotors is two orders of magnitude larger than the body mass  $M_0$ .

### 3. Force Distribution in Locomotion over a Rigid Surface

This section is concerned with the algorithms of computing commanded force distribution in locomotion over a rigid surface. The corrections  $s_*^{(j)}$  to the commanded leg position are assumed to be zero. The distribution of vertical force components in locomotion over a slightly uneven horizontal surface and distribution of vertical and horizontal force components in locomotion within a dihedral angle are considered. In the latter case some simplifying kinematic assumptions are made. Experimental results are presented.

#### 3.1. Force Distribution Algorithms

Since a walking vehicle moves relatively slowly, the influence of dynamic factors on force distribution may be neglected. The commanded forces must be computed proceeding from the body orientation relative to the gravity vector, and from the leg configuration. We use the vehicle body-fixed coordinate system OXYZ. Suppose the surface is slightly uneven and the vehicle body is in the horizontal position; then the OZ axis is collinear to the gravity vector.

Force distribution can be determined by several methods within the framework of static indeterminacy. We consider eliminating indeterminacy by using a certain optimization criterion. Let the vector  $W$  specify the configuration of the legs and the orientation of the vehicle body determined from sensory data. Let  $G$  denote the state vector specifying the set of the supporting legs. Using  $W$  and  $G$  and the optimization

criterion, we can find the "optimum" force distribution

$$N_*^{(j)} = N_0^{(j)}(W, G) \quad (17)$$

In eq. (17)  $N_0^{(j)} = 0$  for the legs that are not in support. The vehicle configuration  $W$  varies slowly enough. But the leg state vector  $G$  varies abruptly with a change of the set of the supporting legs. Therefore, the forces calculated from eq. (17) will also vary abruptly and should not be tracked. So, let us perform a smooth force redistribution during the joint support phase, which separates the transfer phases of different sets of legs.

Let  $G_0$  and  $G_n$  be the states of the vehicle legs before and after the joint support phase, respectively. During the joint support phase, forces must vary smoothly from  $N^{(j)} = N_0^{(j)}(W(t_1), G_0)$  to  $N^{(j)} = N_0^{(j)}(W(t_2), G_n)$ , where  $t_1$  and  $t_2$  are the instants of the beginning and the end of the phase. The part of the control system responsible for force distribution operates independently of the upper level (for example, a supervisory one), which controls the motion of the vehicle body. Therefore, the vehicle configuration at the end ( $t_2$ ) of the joint support phase is unknown beforehand. Nevertheless, a desired force redistribution can be achieved. Assume that during the joint support phase

$$N_*^{(j)} = (1 - \alpha(t))N_0^{(j)}(W(t), G_0) + \alpha(t)N_0^{(j)}(W(t), G_n), \quad (18)$$

where  $\alpha(t)$  is a linear scalar function varying from  $\alpha(t_1) = 0$  to  $\alpha(t_2) = 1$ . The forces calculated from eq. (18) coincide with the required values at  $t_1$  and  $t_2$ , and at any instant satisfy the statics equations, which are linear in forces. Thus in the beginning of the next transfer phase, the legs to be transferred will be unloaded and the transfer will begin without jerks and impacts. It may be supposed that a linear combination of "optimum" distributions given by eq. (18) is quite satisfactory in the sense of the criterion chosen.

To calculate the foot forces, it is necessary to know, in addition to the vehicle weight  $P$ , the coordinates  $X$  and  $Y$  of the vehicle center-of-mass. In most of the known walking vehicles, the mass of the legs amounts to a considerable proportion of the total mass of the vehicle. For this reason  $X$  and  $Y$  depend on the vehicle configuration.

Let

$$\rho^{(i)} = \begin{bmatrix} x^{(i)} - x_0^{(i)} \\ y^{(i)} - y_0^{(i)} \end{bmatrix}$$

be a vector in the  $OXY$  plane that connects the suspension point of the  $i$ th leg with the leg tip. Assuming the leg structure symmetric we may consider the center-of-mass of the leg to lie in the leg plane. Then the vector in the  $OXY$  plane connecting the suspension point with the leg center-of-mass projection  $\rho_c^{(i)}$  is collinear to the vector  $\rho^{(i)}$ , and we may write

$$m_i \rho_c^{(i)} = m_f \rho^{(i)}, \quad (19)$$

where  $m_i$  is the leg mass and  $m_f$  is a scalar depending on the angles in the second and third joints of the leg.

Relation (19) means that the leg is replaced by two mass points:  $m_f$  located at the leg tip, and  $m_i - m_f$  located at the suspension point and rigidly connected with the body. In locomotion with a moderate step, only the angles in the first joints of the legs vary considerably. Therefore, we assume  $m_f = m$  for all the legs.

Thus, the model of mass distribution is: the legs with mass points  $m$  located on the leg ends and the body of mass  $M_c = M - 6m$ , where  $M$  is the total mass of the vehicle.  $X$  and  $Y$  are the coordinates of the center-of-mass. In accordance with this model the right sides in the statics equations are

$$\begin{aligned} P &= (M_c + 6m)g \\ PX &= mg \sum_{i=1}^6 x^{(i)} + M_c X_c g \\ PY &= mg \sum_{i=1}^6 y^{(i)} + M_c Y_c g \end{aligned} \quad (20)$$

Though eq. (20) defines the coordinates of the vehicle center-of-mass in terms of the leg configuration with some error, the advantage is in computational simplicity. The experimentally identified parameters are as follows:  $m = 0.7$  kg,  $M_c = 18$  kg,  $X_c = 2$  cm, and  $Y_c = 0$ .

### 3.2. Distribution of Vertical Force Components

#### Calculation of Commanded Forces

Let the horizontal force components be zero. Then the vertical force components must satisfy the static equilibrium equations

$$\begin{aligned} \sum_{i \in I} N_i^{(i)} &= P \\ \sum_{i \in I} N_i^{(i)} x^{(i)} &= PX \\ \sum_{i \in I} N_i^{(i)} y^{(i)} &= PY, \end{aligned} \quad (21)$$

where  $P$  is the vehicle weight,  $x^{(i)}$ ,  $y^{(i)}$  are the coordinates of the  $i$ th leg tip, and  $X$ ,  $Y$  are the coordinates of the vehicle center-of-mass. Summation in eq. (21) is performed over the set  $I$  of the supporting legs.

Forces in  $n$  supporting legs should satisfy the three equations in (21). It is clear that if  $n > 3$ , the solution may be chosen ambiguously. There are different ways of eliminating the indeterminacy. Let us require that the vertical force components should satisfy

$$\sum_{i \in I} (N_i^{(i)})^2 \longrightarrow \min \quad (22)$$

This condition has the sense of energy optimization (i.e., minimization of energy consumption for supporting the vehicle weight). It has been considered by Klein and Wahavisan (1984). The exact condition of energy optimization is more complex, and consequently the computation of forces becomes more complicated (McGhee, Olsen, and Briggs 1980; Okhotsimsky and Golubev 1984). It should be noted that the forces resulting from criterion (22) are of reasonable values from the viewpoint of the criterion  $\max_i N_i^{(i)} \rightarrow \min$ , which corresponds to locomotion over soil with a limited bearing capacity. Criterion (22) is used mainly because of the computational simplicity of the force distribution problem.

Write out the solution of eq. (21) that satisfies condition (22). Introduce an  $n$ -dimensional vector  $N_i$  composed of the vertical force components; the vector

of right sides of system (21)

$$\mathbf{P} = \begin{bmatrix} P \\ PX \\ PY \end{bmatrix}$$

and a  $3 \times n$  matrix

$$\mathbf{A} = (a_{ij}),$$

where

$$a_{1j} = 1, \quad a_{2j} = x^{(j)}, \quad a_{3j} = y^{(j)}, \quad (j = \overline{1, n}).$$

Then equation (21) may be written in matrix form as  $\mathbf{AN}_z = \mathbf{P}$ . The solution of this equation under condition of (22) is  $N_{z0} = \mathbf{A}^+ \mathbf{P}$  (Gantmacher 1959), where  $\mathbf{A}^+ = \mathbf{A}^T (\mathbf{A} \mathbf{A}^T)^{-1}$  is the pseudo-inverse of the matrix  $\mathbf{A}$ . If three legs are on the support, then the matrix  $\mathbf{A}$  is square and  $\mathbf{A}^+ = \mathbf{A}^{-1}$ . This solution can be obtained by the Lagrange multiplier method, and we represent it as  $N_{z0} = \mathbf{A}^T \mathbf{p}$ , where

$$\mathbf{p} = \begin{bmatrix} p_1 \\ p_2 \\ p_3 \end{bmatrix}$$

is the Lagrange multiplier vector. The latter equation in the coordinate form is

$$N_{z0}^{(j)} = p_1 + p_2 x^{(j)} + p_3 y^{(j)} \quad (23)$$

It is convenient to determine the vector  $\mathbf{p} = (\mathbf{A} \mathbf{A}^T)^{-1} \mathbf{P}$  as a solution of the system  $(\mathbf{A} \mathbf{A}^T) \mathbf{p} = \mathbf{P}$  or in terms of the coordinates

$$\begin{bmatrix} n & S_x & S_y \\ S_x & S_{xx} & S_{xy} \\ S_y & S_{xy} & S_{yy} \end{bmatrix} \begin{bmatrix} p_1 \\ p_2 \\ p_3 \end{bmatrix} = \begin{bmatrix} P \\ PX \\ PY \end{bmatrix} \quad (24)$$

$$S_x = \sum_{i \in I} x^{(i)}, \quad S_y = \sum_{i \in I} y^{(i)}, \quad S_{xx} = \sum_{i \in I} (x^{(i)})^2,$$

$$S_{xy} = \sum_{i \in I} x^{(i)} y^{(i)}, \quad S_{yy} = \sum_{i \in I} (y^{(i)})^2,$$

where  $I$  denotes the set of the supporting legs and  $n$  is their number. To reduce calculations, the solution of

system (24) was written analytically. Note that in calculating the forces by eqs. (23) and (24), the change in the supporting legs set leads only to a change in the summation set  $I$ .

A similar scheme for calculating the vertical force components was suggested by Waldron (1986).

### Experimental Results

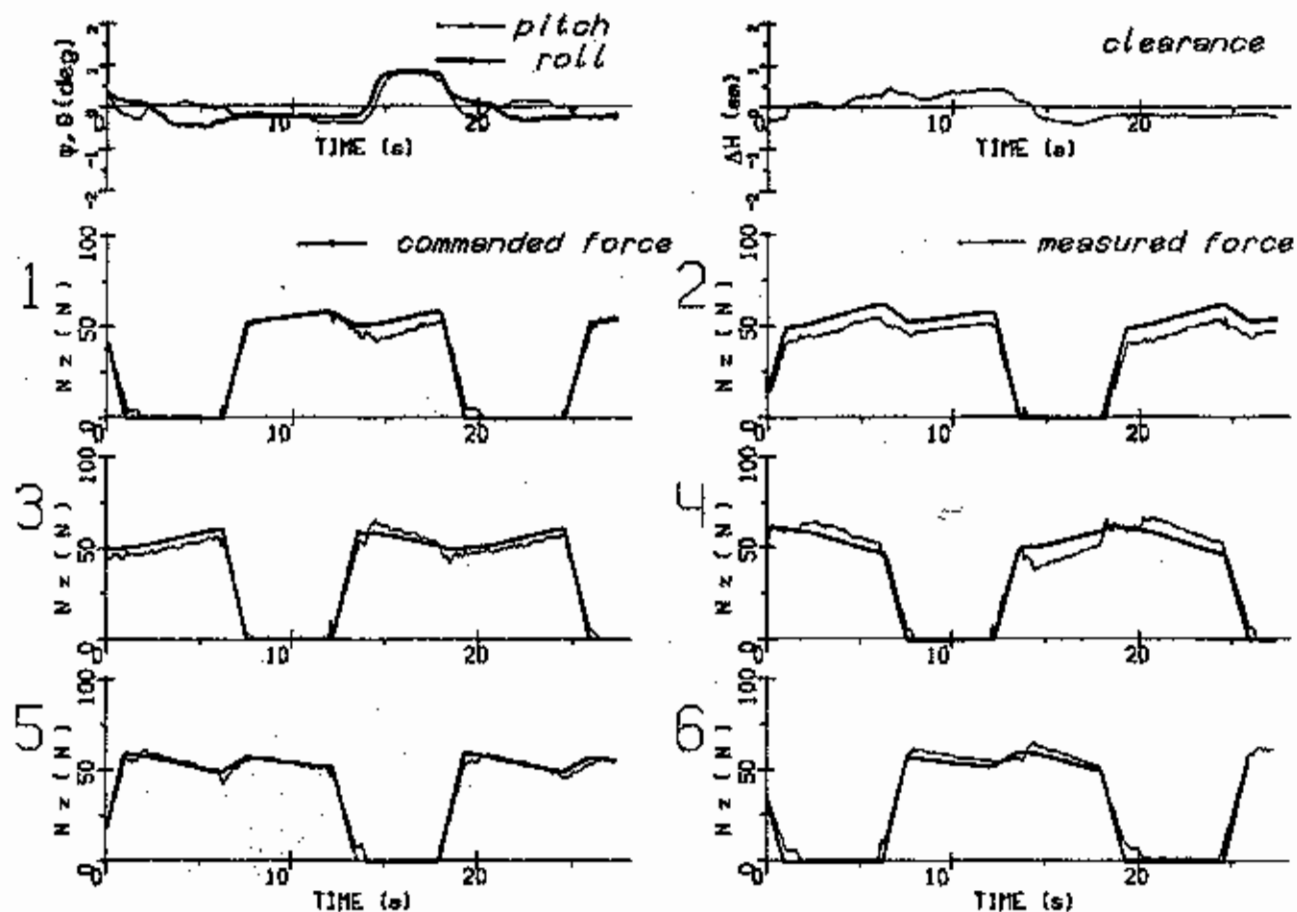
The algorithm of commanded force calculation was implemented on a Nova 2/10 minicomputer connected with the analog computer of the remaining part of the control system via analog to digital converters and digital to analog converters.

Computation of the vertical force component distribution was programmed in FORTRAN-4 with the use of assembler subroutines of vector-matrix arithmetics.<sup>1</sup> It requires about 17 K words of memory and has a cycle time of about 70 ms (this time depends on the gait pattern). The commanded horizontal force components are zero. During the transfer phase, the vertical force components are computed according to eqs. (20), (23), and (24), while during the joint support phase, computations follow eq. (18). The force redistribution described by eq. (18) begins when all the ground contact sensors touch the support.

In the development of force control algorithms, it is necessary to take into account the locomotion cycle properties. Because of various errors and leg structure compliance, contact with the support surface occurs in a later (or earlier) section of the adaptation zone each cycle. This takes place until the vehicle rises (lowers) so that the contact sensors do not operate in the adaptation zone and the locomotion cycle becomes fixed. Such an effect is multiply intensified in the case of actively compliant legs. In this case the vehicle body rises or lowers after several steps. To ensure normal locomotion, it is necessary to correct the linear and angular position of the body with respect to the bearing surface. To this end, control of the vertical velocity ( $v_z$ ), roll velocity ( $\omega_x$ ), and pitch velocity ( $\omega_y$ ) was exercised without displacing the locomotion cycles relative to the body. Correction was made after each step at the beginning of the joint support phase. Linear and

1. These subroutines were written by E. V. Gurfinkel.

Fig. 5. Experimental results in the control of vertical force distribution in locomotion over rigid surface.



angular errors between the bearing surface and the plane through the middles of the adaptation zones of the legs were calculated by the least squares technique using the positions of the leg tips. Vertical and angular velocities of the body were corrected proportionally to these errors.

Measured and commanded forces, as well as clearance, pitch, and roll variations were stored. These experimental results obtained in the locomotion over an even rigid surface with a diagonal gait (1, 6-2, 5-3, 4) are plotted in Figure 5. The vehicle moved forward with a step length of about 10 cm. The position of the plots corresponds to the disposition of the legs on the top view (the numbers of the legs are indicated near the ordinate axes). The plots of the forces, angular displacements of the body, and the clearance in the case of actively compliant legs shows that the algo-

ritms ensure commanded force tracking with a high quality of locomotion.

From Figure 5 it can be seen that during the joint support phase one set of legs is loaded, another is unloaded. Redistribution of loads is smooth, without jumps, as distinct from the situation when forces are not controlled.

### 3.3. Control of Transversal Forces

Now consider a situation when it is necessary to control horizontal force components for the foot forces to be within friction cones. Suppose that the vehicle moves inside a dihedral angle formed by two rigid

Fig. 6. The general view of the vehicle in transversal force control experiments.

planes each making an angle  $\varphi$  with the horizon. The line of intersection of the bearing planes is horizontal. The vehicle body is also horizontal, and the  $OX$  axis of the body coordinate system is parallel to this line. The left and right legs are supported by different planes, with all the supporting points lying in the same horizontal plane.

Demand the contact forces to lie as close as possible to the normals to the bearing planes. It is clear that the longitudinal force components should be zero

$$N_x^{(i)} = 0 \quad (25)$$

and the forces lie in the  $OYZ$  plane.

Six equations of the static equilibrium specify a resultant force vector and a resultant torque to be zero. One of these equations always holds true because the resultant force vector projection onto the  $OX$  axis is zero in accordance with eq. (25). Since the supporting points lie in the same horizontal plane, the three equations with vertical force components are of the form of (21).

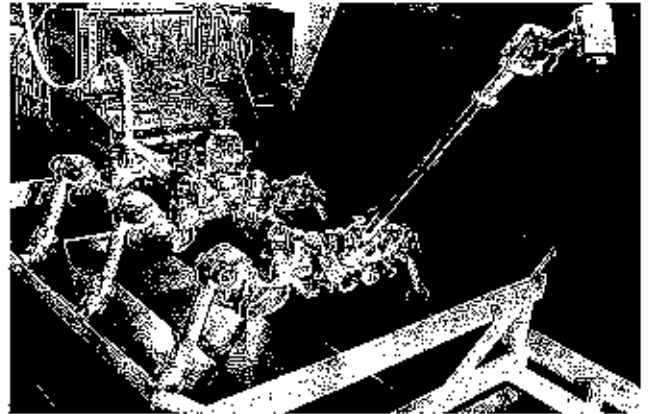
Let us consider a vehicle walking through a tripod gait and assume that the body center,  $O$ , is always above the line of intersection of the bearing planes. Suppose that three legs are on the support. The leg denoted by  $a$  lies on one side from the line of intersection; the legs  $b$  and  $c$  lie on the other side at the same distance. Thus,  $y^{(b)} = y^{(c)} = -y^{(a)}$ . The three equations in (21) uniquely determine the vertical forces  $N_y^{(i)}$ ,  $i \in I$ ,  $I = \{a, b, c\}$ .

The two remaining equations contain the horizontal force components

$$\begin{aligned} N_y^{(a)} + N_y^{(b)} + N_y^{(c)} &= 0 \\ N_y^{(a)}x^{(a)} + N_y^{(b)}x^{(b)} + N_y^{(c)}x^{(c)} &= 0 \end{aligned} \quad (26)$$

Three unknowns enter into the two equations in (26). Thus, the distribution of the transverse forces  $N_y^{(i)}$  depends on one free parameter. For instance, let the force  $N_y^{(a)}$  in a middle leg be chosen as such a parameter. Then solutions of (26) are of the form

$$\begin{aligned} N_y^{(b)} &= -N_y^{(a)} \frac{x^{(a)} - x^{(c)}}{x^{(b)} - x^{(c)}} \\ N_y^{(c)} &= -N_y^{(a)} \frac{x^{(b)} - x^{(a)}}{x^{(b)} - x^{(c)}} \end{aligned} \quad (27)$$



The vehicle may stay on one of the two triples. Let

$$\begin{aligned} N_y^{(a)} &= N_y^{(a)} \operatorname{tg} \varphi, & \text{for } b=1, \quad a=4, \quad c=5 \\ N_y^{(a)} &= -N_y^{(a)} \operatorname{tg} \varphi, & \text{for } b=2, \quad a=3, \quad c=6 \end{aligned} \quad (28)$$

Thus, the force acting on the middle leg is orthogonal to the bearing surface. If the vehicle center-of-mass position satisfies

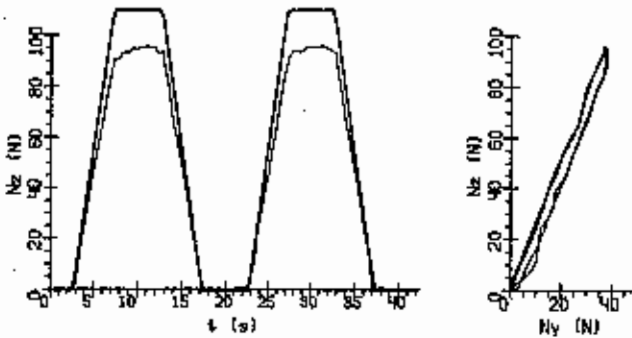
$$X = x^{(a)}, \quad Y = 0 \quad (29)$$

then the forces acting on the legs  $b$  and  $c$  are also orthogonal to the bearing plane. If the coordinates of the center-of-mass slightly differ from their values given by eq. (29), then the forces will not deviate insignificantly from the normal.

Computation of the distribution of the vertical and transverse force components was programmed in FORTRAN-4. The algorithms described in the previous sections were used for calculating the vertical force components. The transverse force components were calculated from eqs. (27) and (28). Force redistribution in accordance with eq. (18) was performed during the joint support phase. The program cycle time was about 90 ms. In experiments the vehicle stamped by a triple gait between two rigid inclined wooden planes (Fig. 6).<sup>2</sup> The angle between each plane and the horizon was  $\varphi = 35^\circ$ . Figure 7 shows the time dependence of the commanded and measured vertical

2. L. V. Saukh took part in these experiments.

Fig. 7. Experimental results for the transversal force control.



components of the force acting on the first leg. The relationship between the vertical and transverse force components for this leg is also presented. It can be seen that as the leg is loaded, the horizontal component increases proportionally to ensure an approximately constant direction of the force vector. The forces in the other legs vary in the same manner.

#### 4. Locomotion over Soft Soil

This section is concerned with the control of the vehicle walking in soft soil. In this case, in addition to the commanded position  $r_c$  and commanded force  $N_c$ , real-time computations also include the commanded leg sinkage  $S_c$  from eq. (2). The computation of the commanded leg sinkage is closely connected with the computation of the commanded force. Note that one of the algorithms considered here corrects leg sinkage in the absence of force feedback.

##### 4.1. Mechanical Properties of Soils

In locomotion over slightly uneven terrain, the horizontal force components are negligible. For this reason we are interested only in the load-sinkage curves. Such curves for a number of soils and synthetic materials were obtained experimentally with the aid of the vehicle leg. All legs but one stayed on a rigid support; the remaining leg was placed on soil or a synthetic mate-

Fig. 8. Load-sinkage curves obtained by the vehicle leg: —, loosened sandy loam; + + +, granulated polyethylene.

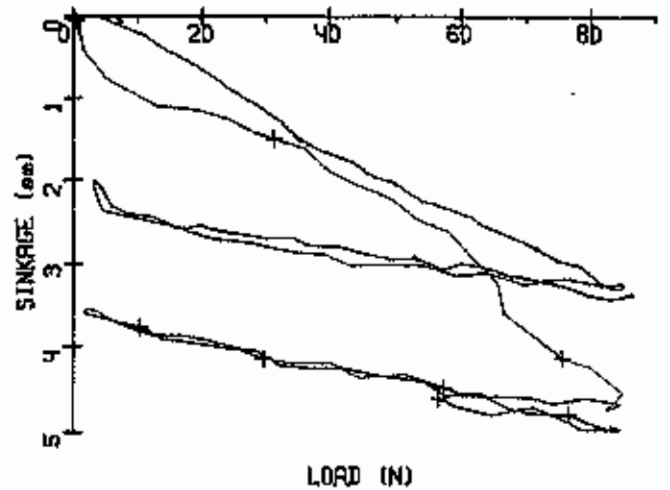
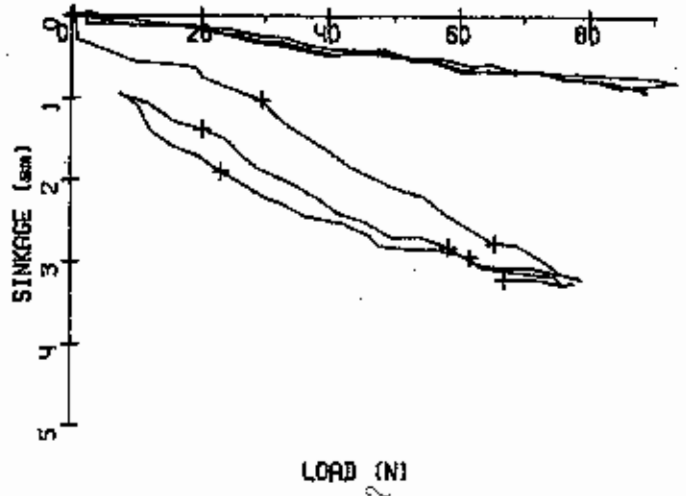


Fig. 9. Load-sinkage curves obtained by the vehicle leg: —, rigid support; + + +, porolon layer.

rial to be investigated. The load on this leg was repeatedly changed from zero to a maximum value (about 100 N) and vice versa. The leg sinkage was determined by means of joint angle sensors, and the load was measured by means of a force sensor. Some of the experimental load-sinkage curves are shown in Figures 8 and 9. A maximum load on the leg was 120 N, with the foot area 30 cm<sup>2</sup>, resulting in a pressure of 40 kPa. Note that the data presented are inaccurate. Figure 9 presents the load-sinkage curve obtained for an absolutely rigid support. The slope of the curve corresponds to the compliance of the vehicle and leg structure.

As seen from Figure 8 and known from the literature (Bekker 1967), in natural soils the sinkage is irrevers-

ible. Synthetic soil of polyethylene granules has similar mechanical properties. For another synthetic material, porolon (porometric polyurethane) (Fig. 9), the load-sinkage relation is almost unambiguous and linear. Thus, we consider only two simplified soil models.

For soils of the first type, all deformations are reversible, and the sinkage depends on load unambiguously. Though such a situation is not widespread in nature, the problem of locomotion over elastic soil is of interest in itself. In the development of algorithms it was assumed that the dependence of the force on the sinkage was the same and known at any point on the terrain.

The second type of soil has completely irreversible deformations. Most natural soils are close to this model. Such a soil behaves as an absolutely rigid support if the load on the foot becomes less than a maximum value already achieved. Note that the properties of natural consolidating soils may differ considerably, even at close points of terrain (Bekker 1967).

#### 4.2. Basic Approaches to Locomotion Control

The simplest way to walk in soft soil is to fix the locomotion cycles. In this case the inhomogeneity of the soil mechanical properties and unevenness of the surface may lead to a considerable disturbance of the vehicle motion.

A more complicated approach is the use of the locomotion cycle with an adaptation zone. In order that a leg should strike the supporting surface in the adaptation zone, it is necessary to stabilize the body position relative to the support (roll, pitch, and clearance) by compensating for leg sinkages. In a simple variant it may be done by keeping the supporting polygon rigid (Okhotsimsky et al. 1985). To obtain comfortable motion, we individually corrected the motion of each leg in accordance with its sinkage.

To correct the body motion and to control leg sinkage, it is necessary to know the body position relative to the bearing surface. For this purpose we used the information on the leg positions relative to the body and on the leg contact with the surface.

#### 4.3. Locomotion over Elastic Soil

First, consider correction algorithms for leg motion that allow for leg sinkage in the case where the mechanical properties of soil are known a priori. Two algorithms of the body motion stabilization were tested in locomotion over an elastic surface (a porolon sheet). Let us assume that the force  $N_i^{(j)}$  depends on the sinkage  $s_i^{(j)}$  of the  $i$ th leg unambiguously

$$N_i^{(j)} = c_s s_i^{(j)}, \quad (30)$$

where soil stiffness  $C_s$  is (known a priori) equal for all the legs.

The first algorithm is based on the force distribution control by means of force feedback. Since the load-sinkage dependence is known a priori, the commanded sinkage  $s_i^{(j)}$  can be computed from the commanded load on the leg.

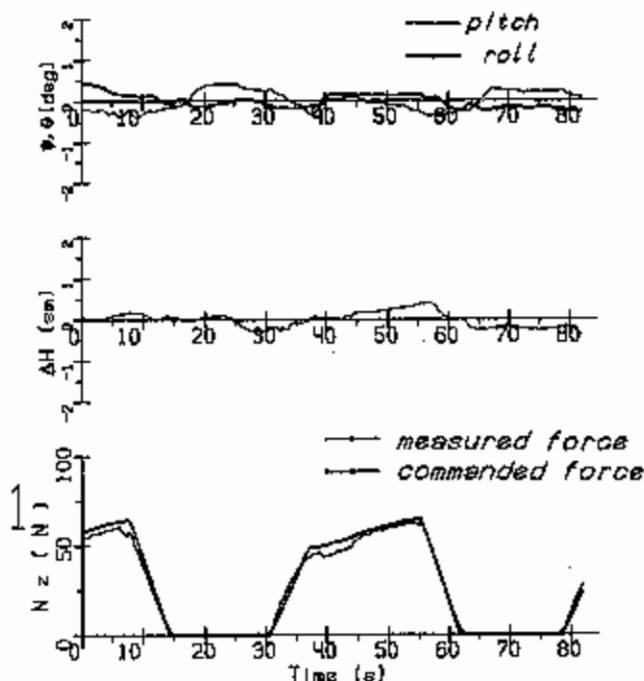
The algorithm was implemented on the basis of the vertical force control algorithm described in section 3.2. The motion of each supporting leg was corrected for its sinkage computed from the commanded force,

$$s_{*i}^{(j)} = N_{*i}^{(j)} / c_s.$$

A porolon sheet about 6 cm thick was used as a model of linearly elastic soil. Its load-sinkage curve is shown in Figure 9. Experimental results for the algorithm are presented in Figure 10. The record is also shown of the commanded and measured vertical force components for one of the legs. The quality of tracking the commanded forces in the remaining legs is similar. The leg sinkage amounted to 5 cm, and variations in the body position are an order of magnitude less. It should be noted that information about the body position obtained by means of a gyro attitude and a proximity sensor was used only for recording but not for control.

The second control algorithm also presupposes that the soil properties are known a priori. The algorithm corrects the motion of each leg with an allowance for its sinkage, and does not use force feedback. The leg sinkage will have commanded values if the corresponding forces satisfy the statics equations. The commanded subsidence of each leg should be determined

Fig. 10. Experimental results for walking in porolon with force feedback and leg sinkage control.



on the basis of the previously computed force distribution.

Such an algorithm was implemented on the basis of the algorithm used to compute commanded force distribution described in section 3.2. In locomotion over elastic soil (30), it was supposed that  $s_z^{(i)} = N_z^{(i)}/c_s$ , where  $N_z^{(i)}$  is the commanded vertical force component.

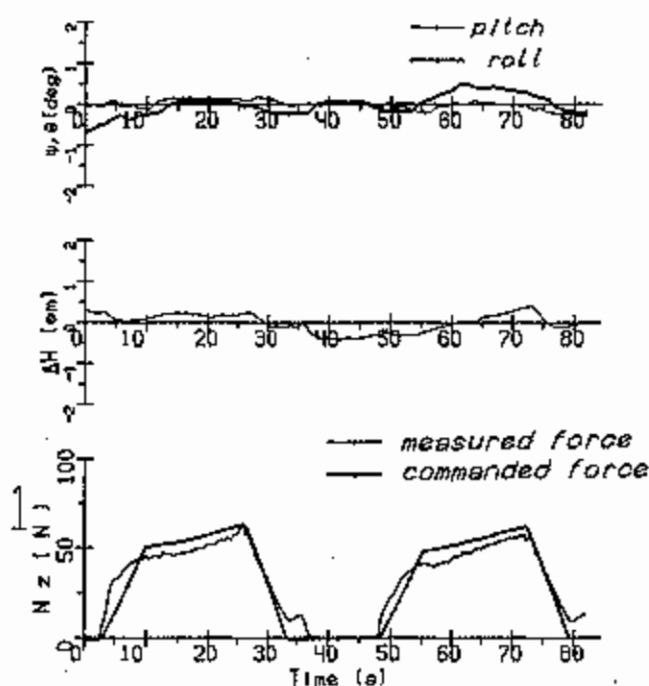
The experimental results for locomotion over the same porolon sheet are presented in Figure 11. As can be seen, the quality of stabilization of the body motion is high, but the commanded forces are tracked worse than in the previous algorithm (Fig. 10).

#### 4.4. Locomotion in Consolidating Soil

Suppose now that the mechanical properties of soil are unknown beforehand. Then the motion of each leg should be corrected for its sinkage, which cannot be computed beforehand but can be only measured.

The following algorithms are based on the assump-

Fig. 11. Experimental results for walking in porolon with leg sinkage control only.



tion that soil deformation is completely irreversible. In this case, if the load on the leg is less than the value once achieved, the leg may be considered to be on a rigid support. The absolute displacement of the body may be determined from these leg positions.

#### Leg Sinkage Control

Let  $\psi$  and  $\theta$  be small deviations of the roll and pitch of the body from its initial horizontal position and  $\Delta H$  be a change in clearance resulting from leg sinkage. Write  $s_z^{(i)}$  for a small vertical displacement of the  $i$ th leg after contact with soil relative to the body. The displacement of this leg in the earth-fixed coordinate system (sinkage) is

$$s_z^{(i)} = \Delta H - \psi x^{(i)} + \theta y^{(i)} + s_z^{(i)} \quad (31)$$

Let us assume that  $n$  ( $n \geq 3$ ) legs are on absolutely rigid soil. For these legs,  $\sigma_z^{(i)} = 0$ , and eq. (31) may be used to determine the angular ( $\psi, \theta$ ) and linear ( $\Delta H$ ) displacements of the body. The equations for determining the body displacement have the matrix form  $A^T s = q$ , where  $s = (s_z^{(1)}, s_z^{(2)}, \dots, s_z^{(n)})^T$  is the dis-

Fig. 12. Experimental results for foot force control for consolidating soil.

placement vector of the legs that are on the rigid support, and the vector  $q = (-\Delta H, \psi, -\theta)^T$  specifies the body displacement. The matrix  $A$  of size  $n = 3$  is of the form  $A = (a_{ij})$ , where  $a_{1k} = 1$ ,  $a_{2k} = x^{(k)}$ ,  $a_{3k} = y^{(k)}$ , ( $k = 1, n$ ),  $x^{(k)}$ ,  $y^{(k)}$  are the coordinates of the tips of the legs on the rigid support.

The best mean-square evaluation of the body displacement  $q$  from these equations is provided by the formula

$$q = (A^T A)^{-1} A^T s.$$

It is convenient to seek  $q$  as the solution of the equivalent equation

$$(A^T A)q = A^T s,$$

which, if written in components, is of the form

$$\begin{pmatrix} n & S_x & S_y \\ S_x & S_{xx} & S_{xy} \\ S_y & S_{xy} & S_{yy} \end{pmatrix} \begin{pmatrix} -\Delta H \\ \psi \\ -\theta \end{pmatrix} = \begin{pmatrix} D \\ D_x \\ D_y \end{pmatrix} \quad (32)$$

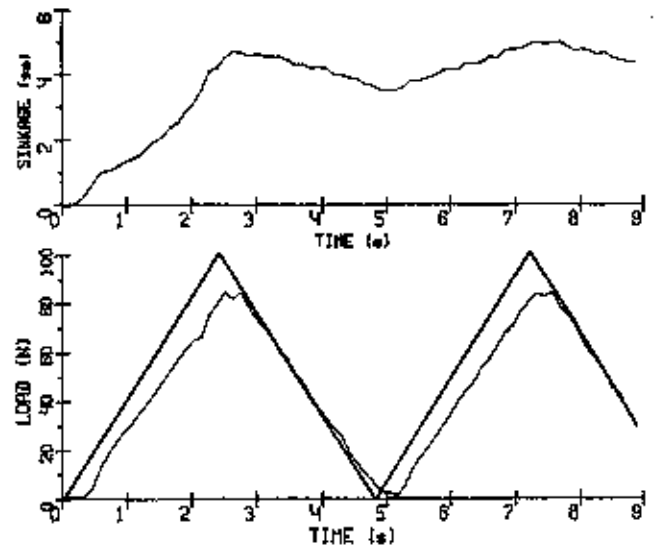
$$D = \sum_{j \in H} s_j^{(j)}, \quad D_x = \sum_{j \in H} s_j^{(j)} x_j^{(j)}, \quad D_y = \sum_{j \in H} s_j^{(j)} y_j^{(j)},$$

where  $H$  is the set of the indices of the legs on the rigid surface. The expressions for  $S_x, S_y, S_{xx}, S_{xy}, S_{yy}$  are the same as in eq. (24) if the set of summation  $I$  is substituted by  $H$ .

During the redistribution of loads on the legs the sinkage of the legs standing on soft soil will increase. The sinkage of each of these legs can be found by eq. (31), using information on the position sensors. For this purpose it is necessary to determine the body displacement by solving system (32). To stabilize the body and maintain the prescribed foot forces in spite of leg sinkage, we set the change in the commanded position of the  $i$ th leg in each control cycle equal to the actual sinkage

$$s_{iz}^{(i)} = \sigma_z^{(i)} \quad (33)$$

With such an algorithm, the sinkage will increase until the foot force becomes close to the commanded value. The described algorithm (31)-(33) was implemented on a computer and checked experimentally.



All legs of the vehicle except the first leg stood on a rigid support. The first leg was in soft soil (a layer of polyethylene granules about 8 cm thick, with the granule diameter being 4 mm).

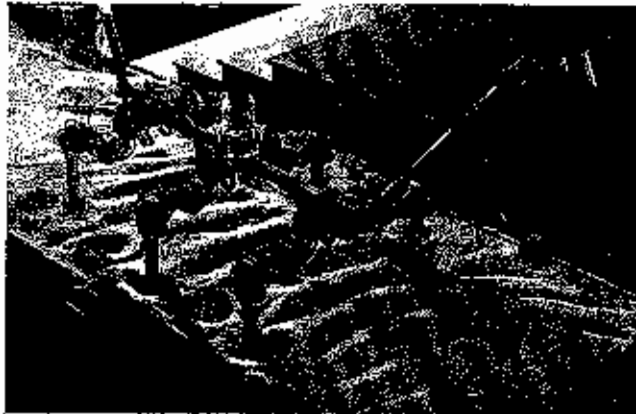
Force distribution was specified in such a manner that, for the commanded forces satisfying eq. (21), the load on the first leg varied from zero to a maximum value (about 120 N). The experimental time dependences of the commanded and measured forces and of the sinkage are shown in Figure 12. The quality of tracking the commanded forces was high enough in spite of a considerable leg sinkage.

#### Locomotion by Tripod Gait

In locomotion by tripod gait, the loads on the three supporting legs during the transfer phase are defined unambiguously. Let us organize a uniform force redistribution during the joint support phase as described in section 3. Then during the joint support phase, the loads on the legs of the one tripod gradually fall off to zero. This tripod may be considered standing on a rigid support, and we may use these legs to determine the body displacement. At the same time, the legs of the other tripod are being loaded and sunk in accordance with the algorithms described in the previous section.

To ensure normal locomotion, a leg should meet

Fig. 13. Photograph of the vehicle during tripod gait walking in consolidating soil.



the bearing surface in the adaptation zone. For this purpose it is necessary to maintain the correct position of the body relative to the surface by controlling the angular ( $\omega_x$  and  $\omega_y$ ) and vertical  $v_z$  velocities of the body. Since in the general case the bearing surface is not planar, we demand that the sum of the squared deviations of the middle points of the adaptation zones from the bearing surface should be minimum. Let us write  $z^{(j)}$  for the body-fixed vertical coordinate of the  $j$ th leg (the leg is considered to be supporting). Let  $z_c^{(j)}$  be the desired vertical coordinate (that of the middle of the adaptation zone).

For the sum of the squared deviations of  $z^{(j)}$  from  $z^{(j)} + s_z^{(j)}$  to be minimum, the body displacement  $\Delta H$ ,  $\psi$ , and  $\theta$  should satisfy eq. (32), in which  $s_z^{(j)} = z^{(j)} - z_c^{(j)}$ . The angular ( $\omega_x$ ,  $\omega_y$ ) and linear ( $v_z$ ) velocities of the body were taken proportional to the corresponding desired displacements:

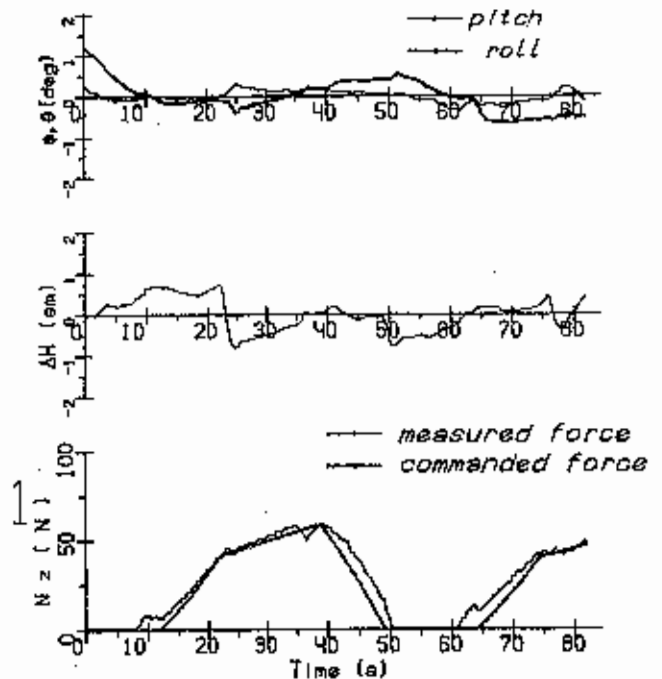
$$v_z = -k_z \cdot \Delta H, \quad \omega_x = -k_\psi \psi, \quad \omega_y = -k_\theta \theta.$$

In experiments the gains  $k_z$ ,  $k_\psi$ , and  $k_\theta$  were taken to be approximately equal to  $4/T_t$ , where  $T_t$  is the duration of the transfer phase.

At the beginning of the joint support phase, the body motion should have ceased, because the algorithm controlling leg sinkage tends to stabilize the body (i.e., prevent its displacement with respect to roll, pitch, and clearance).

The FORTRAN program that implements the above algorithm requires about 20 K. of memory and has a cycle time of 140 ms. In experiments the vehicle

Fig. 14. Experimental results for tripod gait walking in consolidating soil.



walked with a tripod gait in a layer of polyethylene granules about 6 cm thick, with a granule diameter of 4 mm. The load-sinkage curve for this soil is shown in Figure 8.

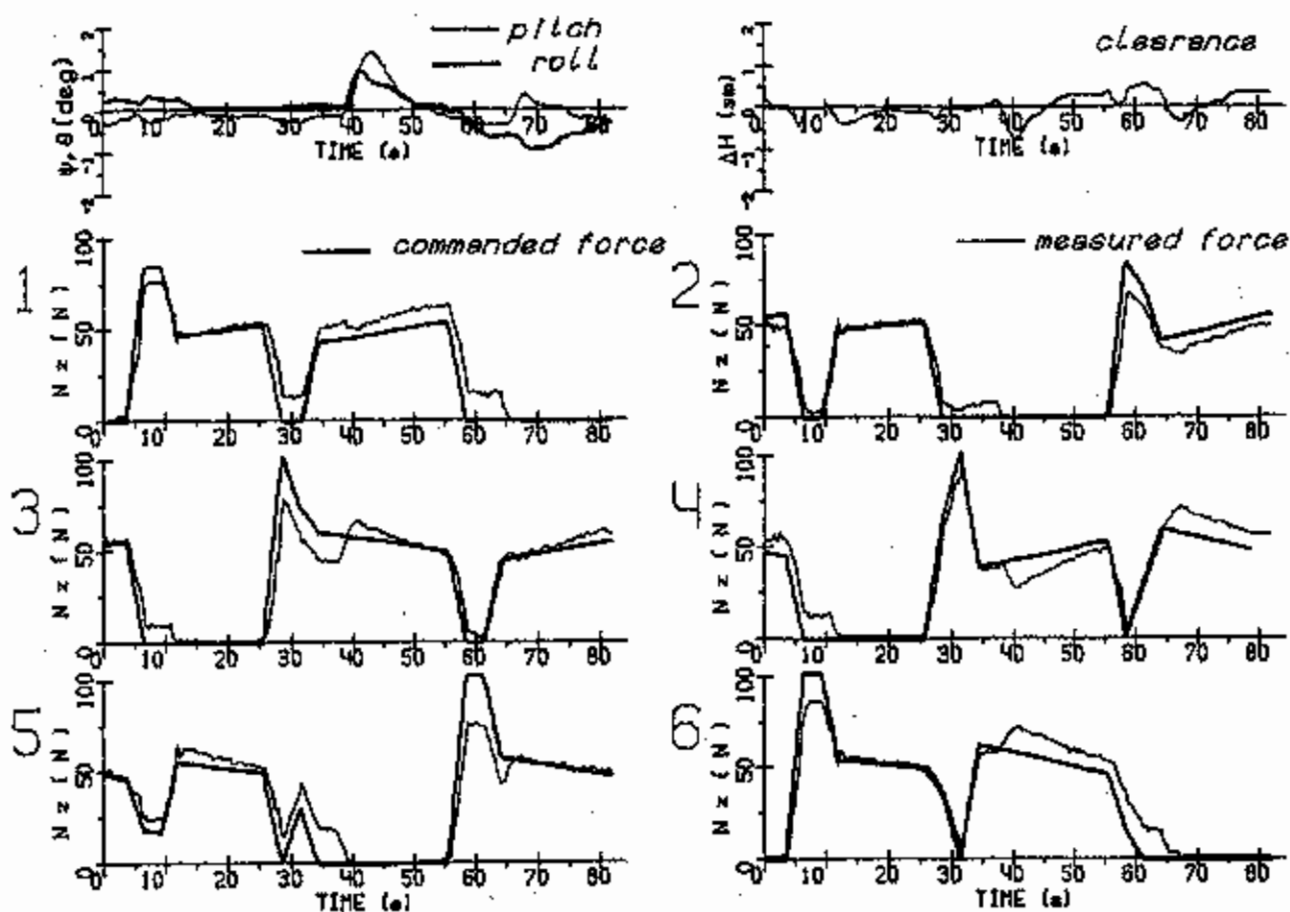
A photo of the vehicle in the experiment is shown in Figure 13. The experimental results are presented in Figure 14. The quality of tracking commanded forces and the stabilization of roll, pitch, and clearance is high. For instance, clearance variation is less than 1 cm with a leg sinkage of about 5 cm, and pitch and roll variations do not exceed 1 grad.

#### Walking with Soil Consolidation

In the case of the control algorithm at the transfer phase (considered in the previous section), when leg sinkage is not controlled, the load on the legs may rise because of the displacement of the vehicle center-of-mass. This may lead to an uncontrollable downfall of the legs into soil and even to the "landing" of the vehicle body on soil, or loss of stability if some of the legs sink to a large extent.

To circumvent this drawback, a walking algorithm with soil consolidation was developed. During the

Fig. 15. Experimental results for diagonal gait walking in consolidating soil.



joint support phase, an intermediate loading of each leg is performed to make contact with soil up to a maximum achievable load. In this case leg sinkage may exceed the permissible value only at the joint support phase when the body position is controlled by the remaining legs standing on the consolidated soil.

It can be shown that the load on a given leg is maximum when the vehicle stands on three legs, including the given one. The supporting triples corresponding to a maximum loading of each newly placed leg are determined at the beginning of the joint support phase. The latter is divided into  $K + 1$  equal time intervals, where  $K$  is the number of newly placed legs. During the first  $K$  intervals, the forces are smoothly redistributed according to eq. (18) to load each newly placed leg. Within the last interval, the legs to be transferred are unloaded.

In other respects this algorithm is similar to that described in the previous section. During the joint support phase, the tips of the legs standing on the pre-consolidated soil are considered to be motionless, and the position of the legs being loaded is corrected. During the transfer phase, the body position is corrected. The difference between the FORTRAN program implementing this algorithm and that described in the previous section is in the addition of a few new units. Figure 15 presents the records obtained under the same experimental conditions as in the preceding section. The vehicle moved using a diagonal gait (1, 6-2, 5-3, 4) with a step length of about 10 cm.

When several of the legs are transferred, force distribution is similar to that shown in Figure 5. Since two legs are put on soil at a time, the joint support phase is divided into three parts: consolidation of soil under

each of the two legs and transition to the final state (i.e., unloading the legs to be transferred). A decrease in load on each leg in the middle of the support phase corresponds to force redistribution during soil consolidation under the legs that are being placed at that time.

As can be seen the quality of commanded force tracking and of stabilization of body motion is good.

## Conclusion

The part of the control system of a six-legged walking vehicle that ensures force control in locomotion over rigid and soft bearing surfaces has been developed and experimentally tested. Force control is based on force feedback.

A mathematical model of the vehicle dynamics in the presence of force feedback has been developed and is in agreement with experiment. A number of algorithms of commanded force computation have been designed.

A high quality of tracking commanded forces has been achieved in experiments because of a small (less than 1 ms) delay in the force feedback loop closed with the aid of a special analog unit. The time required for computing commanded forces, 140 ms, is far less than the locomotion cycle time.

During locomotion in soft soil, force control is closely related to the correction for leg sinkage. In a simpler case where the soil properties are known a priori, the correction of leg position is computed on the basis of the commanded force, with the quality of locomotion in experiment being high. The quality of motion is somewhat worse if the soil properties are unknown beforehand. In this case the algorithms include the computation of leg sinkage under the assumption of soil consolidation.

In all cases variations of the body motion were 3–10 times less than leg sinkage. The reliability of determining the moment of the leg's contact with the surface considerably influences the quality of the operation of the algorithms developed.

## Acknowledgments

This research was started at the initiative of Professor V. S. Gurfinkel. It was supported by D. E. Okhotsimsky, associate member of the USSR Academy of Sciences, and by Professor E. A. Devjanin.

The authors express their gratitude to the creators of the IPIT-IM hexapod and the control system [E. V. Gurfinkel, A. V. Lensky, L. G. Shtilman, and D. W. Zhikharev (Cand. Sci. Phys-Math)] for their help in experiments.

## References

- Bekker, M. C. 1967. *Introduction to Terrain-Vehicle Systems*. Ann Arbor: University of Michigan Press.
- Devjanin, E. A., Kartashov, V. A., Lensky, A. V., and Shneider, A. Yu. 1982. Force feedback in the control system of a walking vehicle. In *Investigation of Robotic Systems*. Moscow: Nauka, pp. 147–159 (in Russian).
- Devjanin, E. A., et al. 1983. The six-legged walking robot capable of terrain adaptation. *Mech. Mach. Theory* 18(4):257–260.
- Devjanin, E. A., et al. 1987. Control of adaptive walking robot. *Preprints 10th World IFAC Congress, Munich*, 4:218–225.
- Gantmacher, F. R. 1959. *The Theory of Matrices*. New York: Chelsea.
- Gorinevsky, D. M., and Shneider, A. Yu. 1987. Dynamics of small motions of a walking robot when there is feedback with respect to the support reactions. *Mech. Solids* 22(6):37–46.
- Gurfinkel, V. S., et al. 1981. Walking robot with supervisory control. *Mech. Mach. Theory* 16(2):31–36.
- Gurfinkel, V. S., Gurfinkel, E. V., Devjanin, E. A., Efremov, E. V., Zhikharev, D. N., Lensky, A. V., Shneider, A. Yu., and Shtilman, L. G. 1982. Laboratory model of a six-legged walking vehicle with supervisory control. In *Investigation of Robotic Systems*. Moscow: Nauka, pp. 98–147 (in Russian).
- Klein, Ch. A., and Briggs, R. L. 1980. Use of active compliance in the control of legged vehicles. *IEEE Trans. Sys. Man Cybernet.* SMC-10(7):393–400.
- Klein, Ch. A., and Wahavisan, W. 1984. Use of a multiprocessor for control of a robotic system. *Int. J. Robot. Res.* 1(2):45–59.

- 
- McGhee, R. B., Olson, K. W. and Briggs, R. L. 1980. Electronic coordination of joint motions for terrain-adaptive robot vehicles. *Proc. 1980 SAE Auto. Eng. Congr.*, Detroit, pp. 1-7.
- Okhotsimsky, D. E., Golubev, Yu. F. 1984. *Mechanics and Control of a Walking Vehicle*. Moscow: Nauka (in Russian).
- Okhotsimsky, D. E., et al. 1985. Mathematical modelling of the dynamics of a walking robot accounting for soil deformation. Preprint, Keldysh Institute for Applied Mathematics of the USSR Academy of Sciences, No. 152, Moscow (in Russian).
- Tikhonov, A. N. 1952. Systems of differential equations with small parameters at derivatives. *Math. USSR Sbornik* 31(3):575-586 (in Russian).
- Waldron, K. J. 1986. Force and motion management in legged locomotion. *IEEE J. Robot. Automat.* RA-2(4):214-220.
- Whitney, D. E. 1977. Force feedback control of manipulator fine motions. *Trans. ASME J. Dyn. Sys. Meas. Control* 99(2):91-97.